International Journal of Science, Technology, Engineering and Mathematics
Volume 3 Issue 4 December 2023
DOI: https://doi.org/10.53378/353024

Evaluating the Effectiveness of Proportional Nodes Method in Curve Fitting for Surfaces: Application to Data of Dynamic Viscosity of Ammonia-Water Solution

[1]S. N. Mumah, [2]H.F. Akande, [3]S. Alexander, [4]K.Y. Mudi,

[5]O. Olaniyan & [6]F. Samuel

Abstract

This study used the proportional nodes method, a novel curve fitting approach to correlate data for dynamic viscosity of ammonia-water solution. The approach integrates polynomial equations, generated at various temperatures, with those calculated at selected mole fraction nodes. These nodes are scaling factors that account for variations in dynamic viscosity at different temperatures at selected mole fractions. The accuracy of the polynomial equations ensures a high degree of fitting accuracy. The proportional nodes, computed systematically, were integrated into a robust and highly accurate polynomial model to generate correlations that fit the data for the surface. This model exhibited minimal average percentage differences between predicted and actual viscosity values (±0.2614293 for temperature range, 273.15K to 303.15K and ±1.11 for temperature range, 303.15K to 423.15 K), indicating a high level of predictive accuracy. The proportional nodes method offers a significant contribution to both academic research and industry. It provides a more precise and adaptive model for predicting the dynamic viscosity of ammonia-water solution, which is critical for optimizing and designing various industrial applications, including refrigeration systems.

Keywords: *correlations, proportional nodes, curve fitting, dynamic viscosity, ammonia-water solution*

Article History:

***Received**: September 2, 2023* ***Revised**: November 2, 2023*
***Accepted**: November 4, 2023* ***Published online**: November 11, 2023*

Suggested Citation:
Mumah, S.N., Akande, H.F., Alexander, S., Mudi, K.Y., Olaniyan, O. & Samuel, F. (2023). Evaluating the effectiveness of proportional nodes method in curve fitting for surfaces: Application to data of dynamic viscosity of ammonia-water solution. *International Journal of Science, Technology, Engineering and Mathematics*, 3 (4), 1-29. https://doi.org/10.53378/353024

About the authors:

[1]Corresponding author. Director, Centre for Renewable Energy & Chief Lecturer, Department of Chemical Engineering, Kaduna Polytechnic, Kaduna, Nigeria, E-mail: mumahsndoyi@kadunapolytechnic.edu.ng
[2]Chief Lecturer, Department of Chemical Engineering, Kaduna Polytechnic, Kaduna, Nigeria. E-mail: hassan.akande@kadunapolytechnic.edu.ng
[3]Lecturer, Department of Marketing, Kaduna Polytechnic, Kaduna, Nigeria. E-mail: astephen@kadunapolytechnic.edu.ng
[4]Chief Lecturer, Department of Chemical Engineering, Kaduna Polytechnic, Kaduna, Nigeria. E-mail: m.kehinde@kadunapolytechnic.edu.ng
[5]Chief Lecturer, Department of Civil Engineering, Kaduna Polytechnic, Kaduna, Nigeria. E-mail: dejoolaniyan@kadunapolytechnic.edu.ng
[6]Lecturer, Department of Chemical Engineering, Kaduna Polytechnic, Kaduna, Nigeria. E-mail: francissamuel@kadunapolytechnic.edu.ng

1. Introduction

The dynamic viscosity of ammonia-water solution plays a crucial role in numerous industrial applications, particularly in refrigeration systems. Accurately predicting this viscosity is paramount for optimizing and designing such systems. Historically, multiple regression techniques have been extensively employed to understand the relationships between diverse quantities. However, when dealing with multiple variables, especially when fitting data for surfaces, the efficacy of such regression techniques is often challenged. An alternative that garnered attention in this context is the use of polynomials such as Chebyshev Polynomial. Renowned for their numerical interpolation capabilities, Chebyshev Polynomials attempt to emulate a function at multiple points based on a specified polynomial order. While they have proven more accurate than some multi-linear regression methods, challenges arise, especially when handling large datasets. The intricacies further intensify when correlating for surfaces.

This paper seeks to address these challenges by introducing the proportional nodes method in curve fitting. This innovative approach, aiming to construct models with multiple variables, promises a meticulous and systematic method to compute dynamic viscosity. It is designed to overcome the limitations posed by polynomials such as Chebyshev Polynomial. The proportional node method was used to generate correlations for the dynamic viscosity of ammonia-water solution. By integrating polynomial equations generated at various temperatures with those calculated at selected mole fraction nodes, this method aims to offer a more accurate and adaptive model for predicting dynamic viscosity.

This study aims to present a novel method for data fitting which allows models to be constructed with multiple variables on both sides of an equation and which can be computed easily by using a series of least squares regression lines in combination with the equation of the nodes of the various lines at its largest point of dispersion. The underlying principle is finding the best equation of these nodes and the equations of the upper and lower lines. If the equations of the lower and upper lines and that of the nodes of each of the lines are computed accurately, the correlation for the surface can be calculated. This study followed the proportional nodes method introduced by Mumah (2021) in calculating the dynamic viscosity of the ammonia-water solution. In this study, correlations were first developed for the pure components and then used to develop models for ammonia-water solution. The data

generated by these models were compared with values generated from the procedure presented by Conde-Petit (2006).

2. Literature review

Data fitting provides users with a mathematical representation that closely aligns with a sequence of data points, keeping the data's constraints in mind. The curve-fitting process identifies a mathematical formula that best aligns with a designated set of data points by minimizing the difference between the given points and the determined equation. When addressing two or three-dimensional data, the tool of polynomial regression comes into play. At the heart of data analysis lies correlation—a statistical measure that assesses the association between multiple variables. In essence, it examines how closely two variables move in tandem. A positive correlation indicates that as one variable escalates, so does the other and vice versa. Conversely, a negative correlation reveals that as one variable goes up, the other comes down and vice versa. When two variables exhibit no discernible pattern or relationship, it is termed as a neutral correlation (Jaadi, 2019).

Differing from correlation, regression is another pivotal statistical method. It foresees the probable value of a dependent variable (Y) rooted in the known values of one or more independent variables (X), utilizing a fitting equation. This approach aims to fathom the connections between a result variable (Y) and its predictor variable(s) (X), as highlighted by Yang (2017). Notably, understanding correlation can pave the way for accurate predictions. Stanovich (2007) reported that numerous scientific propositions are structured around correlations or their absence, making correlation-centric studies pivotal to these theories. Under feasible conditions, evidence gleaned from correlation studies can be subjected to rigorous experimental testing. In the spheres of science and engineering, correlations play an indispensable role in ascertaining the trustworthiness and accuracy of various measurements. Understanding that a statistical bond between two variables does not automatically imply a cause-and-effect relationship is imperative. There are scenarios where one variable's movement could influence another, or a third distinct factor could impact both (Rajiv et al., 2019).

The meticulous determination of data correlations is quintessential for the systematic design, simulation, and fine-tuning of chemical processes. In certain instances, obtaining

experimental data proves challenging, prompting researchers to turn to manufactured data. While such data has its merits in societal experiments, its application is relatively restricted in scientific and engineering research (Petricioli et al., 2020). Delving deeper, Banerjee and Hero (2016) introduced a sequential testing mechanism for pinpointing and isolating hubs within a correlation graph. Their approach tackled situations where variables, initially unrelated, underwent sudden correlation shifts due to unforeseen events. The expansive applications of this methodology span fault identification, anomaly tracking, and even shifts in time series or financial datasets.

The dynamic viscosity of ammonia-water solution is a key property necessary for design and optimization purposes of refrigeration systems. Numerous studies have been conducted to develop and evaluate different methodologies to understand the dynamic viscosity of ammonia-water better solutions. While several correlation-generating methods for data fitting exist, each brings a unique degree of complexity and accuracy. Viscosity is one of the thermodynamic properties necessary to design and simulate flow equipment and systems. Viscosity can be considered the energy that makes a fluid flow as the molecules interact. Generally, viscosity decreases with increasing temperature in liquids and increases with increasing temperature in gases. Because of this property's role in the design and simulation of flow systems, various correlations have been developed to express the relationship between it and temperature. For gases, pressure also becomes a factor. One of the areas where accurate viscosity values play an important factor is the design and simulation of ammonia-water absorption refrigeration. Poor design, verification or simulation emanating from wrong or inaccurate viscosity values result in inefficient processes or products that do not meet specifications.

Ma et al. (2022) delved into the calibration of the viscous boundary’s adjustment coefficient based on the water cycle algorithm, aiming to enhance the accuracy of dynamic response analysis. Their study incorporated the conventional viscous boundary theory into particle discrete elements through programming. Their model, employed in the seismic response analysis of a rockfill slope, authenticated the calibration's precision and the feasibility of the viscous boundary. While the research provides insights into viscous boundaries, it lacks a direct correlation with ammonia-water solution viscosity and offers no mention of the proportional nodes method, indicating a potential gap in the literature.

In another study, Bhattacharjee et al. (2022) showcased a novel approach for real-time viscosity measurements using a differential pressure sensor system. While their model can measure viscosity changes, the research predominantly focused on water and glycerol mixtures, and there was no apparent applicability to ammonia-water solutions or any reference to the proportional nodes method. Similarly, Rezaei et al. (2022) proposed a model that combines the radial basis function neural network with ant colony optimization, specifically for gas viscosity estimations under high-pressure and high-temperature conditions. Though the research presented a commendable model with high accuracy, its specific application to gases renders it tangential to the context of ammonia-water solutions. Moreover, the proportional nodes method is conspicuously absent.

There are numerous studies conducted on viscosity but majority of them have different focus. For example, Thol and Richter (2021) critically reviewed dynamic viscosity models of binary fluid mixtures, emphasizing asymmetric mixtures. They assessed several models, such as the extended corresponding states method, entropy scaling approaches, and the friction theory, pointing out inherent shortcomings in both experimental data and modelling techniques. Melaibari et al. (2021) centred on predicting the viscosity behaviour of hybrid nano-antifreeze solutions using the Artificial Neural Network and the Response Surface Method. Even though the research provided accuracy metrics and comparisons between methods, the focus was on nanofluids. Similarly, Rahmanifard et al. (2021) advocated for supervised machine learning algorithms in predicting gas component viscosity. Despite the impressive accuracy of their proposed model, their research is confined to gas component viscosities. Barkhordar et al. (2021) took a statistical lens towards nanofluid viscosity correlations, aiming to determine their relationship with variable parameters. While their study provides insights into the accuracy and reliability of certain correlations for nanofluids, it does not directly pertain to ammonia-water solutions. This is similar to Kumari et al. (2021) who investigated the peristaltic transport of fluid, focusing on bile flow in ducts. Their in-depth exploration of linear and nonlinear viscosity variations offered insights into bile's behaviour. Still, with its specificity to bile and the absence of any exploration its direct relevance is minimal. Furthermore, Abbas et al. (2021) focused on ammonia flow boiling in a vertical tube bundle, particularly on a dimple tube's performance. This research is tangentially related due to its focus on ammonia, but it centred on heat transfer coefficients.

Dolomatov et al. (2020) introduced a QSPR model to forecast the dynamic viscosity of saturated arenas vapors. Their model adeptly links dynamic viscosity to molecule descriptors. However, the focus is on vapours and so its relevance is limited.

There are several studies that addressed temperature-dependent viscosity. For instance, Ahmed et al. (2020) and Jouenne and Heurteux (2020) delved into the influence of temperature-dependent viscosity on specific flows, with the former focusing on carbon nanotubes-based nanofluid and the latter on HPAM solutions. Wahab et al. (2020) also investigated the effects of temperature-dependent viscosity flow of a non-Newtonian fluid. Their numerical analysis scrutinized various parameters, shedding light on how they impact velocity, temperature, and concentration profiles. The study of Ahmadi et al. (2019) emphasized temperature as dominant factor affecting the dynamic viscosity of nanofluids by applying three algorithms (ANN-MLP, MARS, and MPR) and found that ANN-MLP had the highest R^2 value of 0.9998, closely followed by MARS and MPR. The most significant finding was the elevated importance of temperature in predicting viscosity when compared to other parameters such as size and concentration. Meanwhile, Irani et al. (2019) found that the viscosity of nanofluid samples displayed non-Newtonian behaviour in alignment with the Power law model, hence, it was proposed mathematical correlations based on temperature and volume fraction. Despite the paper's relevance in discussing curve fitting, if focused on a different type of fluid.

In another study background, Zare et al. (2019) explored the fluidity equation for various functionalized ionic liquids in assessing the temperature-dependent viscosity of diverse functionalized ionic liquids. They found that this equation accurately represented experimental viscosity data, with the dynamic crossover temperature of new ionic liquids being estimated through its parameters. While this paper's application to the ammonia-water solution is not directly addressed, it does highlight the importance of temperature, a factor relevant to other studies. For this, Zare et al. (2019) proposed two generalized correlations for estimating viscosity in evolving generalized correlations based on Peng-Robinson equation of state. The study confirmed these developed models' significant performance and accuracy in estimating supercritical fluid viscosity. The connection of this study to the ammonia-water solution's viscosity remains less clear, indicating a potential gap in the literature. To address accuracy, Wietecha and Kurzydło (2019) introduced the Stokes

viscometer in the determination of the dynamic viscosity coefficient of the stokes viscometer, where they achieved results aligning closely with literature values. The study hints at potential advancements in accuracy, but the direct relevance to the proportional nodes method for ammonia-water solution viscosity indicates a potential gap in the literature. Similarly, Eberhard et al. (2019) discussed a semi-analytical expression for local viscosity profile using a Carreau-type fluid in the determination of the effective viscosity of non-newtonian fluids flowing through porous media. The model showcases great accuracy without requiring additional input parameters, yet its relation to the review theme remains tangential.

The study of Valderrama et al. (2019) presented a generalized viscosity equation for ionic liquids in correlation and prediction of ionic liquid viscosity and showcased consistent results, outperforming other models in terms of simplicity and accuracy. However, ammonia-water solution was not considered in the study. In another study, Razmara et al. (2019) used Molecular Dynamics Simulation to study the viscosity of a specific water-based nanofluid and proposed a correlation that remains accurate for specific volume fractions. Still, its direct application to ammonia-water solution was not considered, indicating a potential gap in the literature. Manesh et al. (2019) discussed applying Fuzzy inference system and ANFIS to model viscosity. While the model shows acceptable accuracy, its direct relevance to the review theme is not strongly established.

According to Habibi et al. (2019), viscosity models significantly influence flow and temperature distributions. For instance, Miyara et al. (2019) introduced the tandem capillary tube method with reliability verified by comparing measured viscosities with reference values. However, the relevance to the current study is not clearly stated, indicating a potential gap in the literature. Moreover, Udawattha et al. (2019) developed a new correlation that effectively expresses the viscosity of various nanofluids while Jayeoba and Okoya (2019) derived analytical solutions for a third-grade fluid flow. While the papers present in-depth analytical solutions, their direct relevance to the current study is not extensively detailed.

3. Methods

This study evaluates the effectiveness of the proportional nodes method in curve fitting, specifically targeting the prediction of dynamic viscosity of an ammonia-water

solution over varying temperatures and mole fractions. The research method used was quantitative approach based on a novel curve-fitting technique. The dynamic viscosity data of ammonia-water solution as presented by Conde-Petit (2006), are used. Polynomial equations are formulated across various temperatures, incorporating them with calculations at specific mole fraction nodes. These nodes, termed as proportional nodes, act as scaling factors, accounting for variations in dynamic viscosity across different temperatures at selected mole fractions.

The proportional nodes method is utilized to correlate the dynamic viscosity data of ammonia-water solution. The model is validated by comparing predicted viscosities of the ammonia-water solution with the actual values, emphasizing R^2 values nearing 1 and minimal deviations between predicted and real data. The R^2 values associated with each equation and the average percentage deviations for two temperature ranges (273.15K to 303.15K and 303.15K to 423.15K) are investigated. The consistency of the model's predictions with the actual data is established by tabulating percentage differences. The findings are related to existing literature, particularly the established relationship between temperature and viscosity in fluid dynamics. The advantages of the new method over traditional polynomial fitting techniques are examined.

4. Results

In this study, the dynamic viscosity values of an ammonia-water solution presented by Conde-Petit (2006) were used. They are tabulated in Table 1, which clearly depict a decrease in dynamic viscosity as the temperature increases for various mole fractions. This is a common behaviour observed in fluids where an increase in temperature tends to reduce the internal resistance to flow, thereby reducing the viscosity (Lide, 2005).

Table 1
Dynamic viscosity of ammonia-water solution for various temperatures and mole fraction

T (K)	Mole fraction (-)										
	0	**0.1**	**0.2**	**0.3**	**0.4**	**0.5**	**0.6**	**0.7**	**0.8**	**0.9**	**1**
273.15	1.749 E-03	2.122 E-03	2.363 E-03	2.301 E-03	1.970 E-03	1.500 E-03	1.027 E-03	6.492 E-04	3.971 E-04	2.478 E-04	1.631 E-04
283.15	1.328 E-03	1.596 E-03	1.771 E-03	1.728 E-03	1.490 E-03	1.147 E-03	7.982 E-04	5.152 E-04	3.233 E-04	2.073 E-04	1.367 E-04
293.15	1.012 E-03	1.201 E-03	1.326 E-03	1.297 E-03	1.128 E-03	8.811 E-04	6.258 E-04	4.144 E-04	2.678 E-04	1.769 E-04	1.168 E-04
303.15	7.819 E-04	9.134 E-04	1.002 E-03	9.834 E-04	8.651 E-04	6.878 E-04	5.004 E-04	3.411 E-04	2.274 E-04	1.547 E-04	1.023 E-04

Generally, data are not depicted into 2 forms in published papers, but this paper argues the necessity to do so. The variation of dynamic viscosity of ammonia-water solution for various mole fractions, *x*, and temperatures is shown in figure 1.

Figure 1

Variation of dynamic viscosity of ammonia-water solution for various mole fraction and temperatures

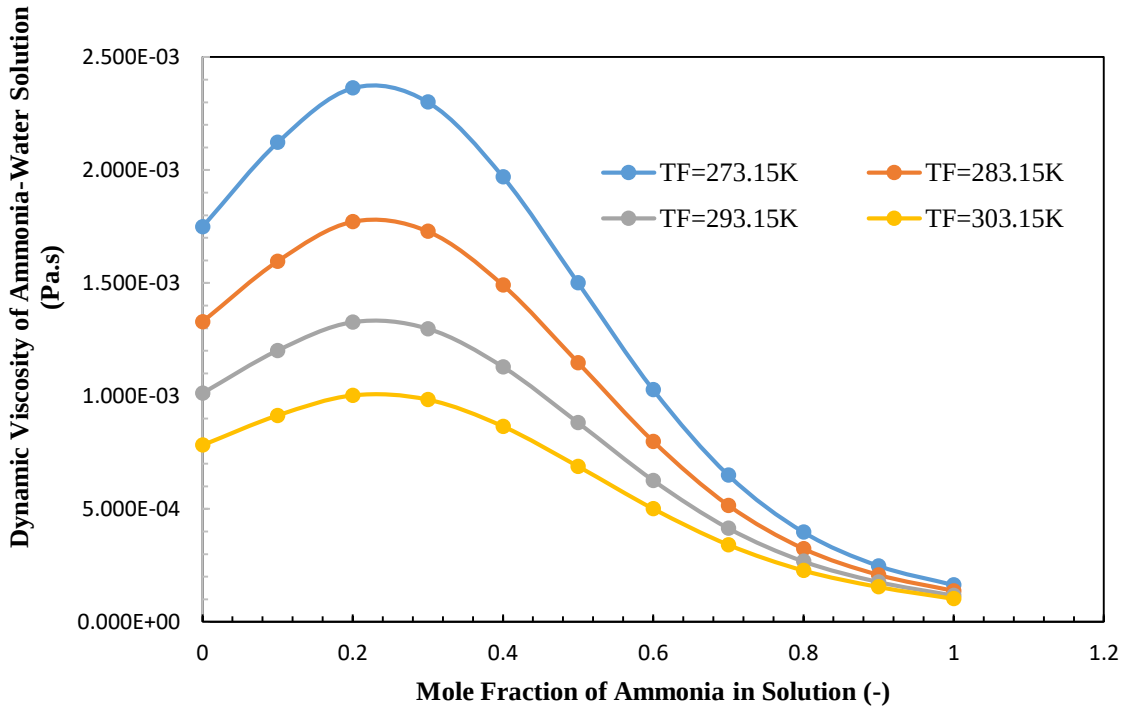

The next step is to generate polynomial equations for each curve as shown in figures 2 to 5. The polynomial equations and coefficient of determination, R^2, generated by Microsoft Excel as shown in table 2, provided a high degree of fitting accuracy, as indicated by R^2 values very close to 1. These R^2 values range from 0.999663 to 0.99985, indicating that over 99.96% of the variation in dynamic viscosity can be explained by the variation in the mole fraction of ammonia in the solution for a given temperature. This high degree of fit is consistent with the previous studies on the viscosity of ammonia-water mixtures (Kumar & Gardas, 2010).

The equations generated for each temperature show that a fifth-order polynomial was used to fit the data. The choice of a fifth-order polynomial, as maintained across different temperatures, is guided by the R^2 values as per the analysis. It is observed that the

coefficients of the polynomials change with temperature, which is a logical outcome, considering that temperature is a fundamental factor affecting viscosity.

Figure 2

Equation at T = 273.15K

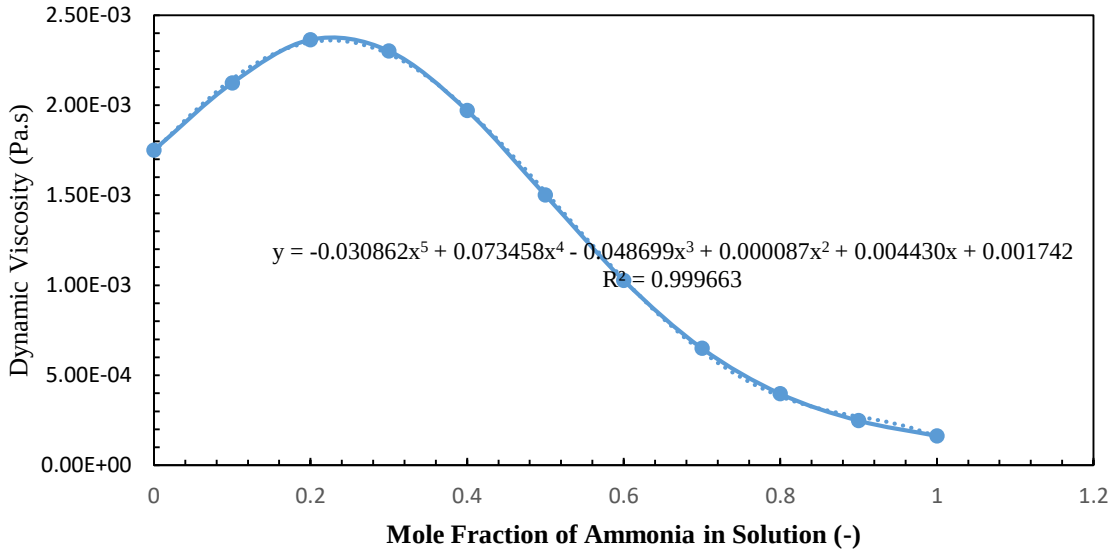

Figure 3

Equation at T = 283.15K

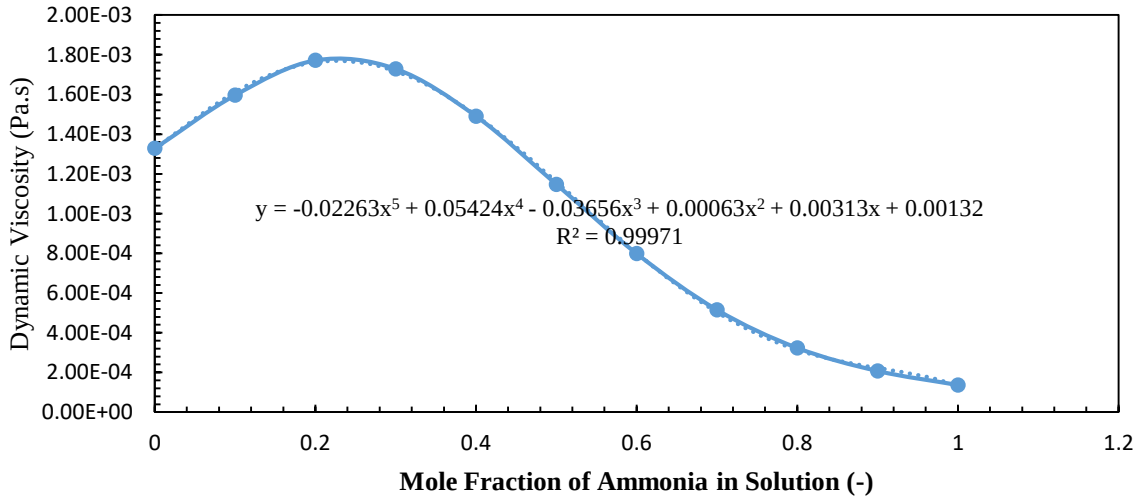

Figure 4

Equation at T = 293.15K

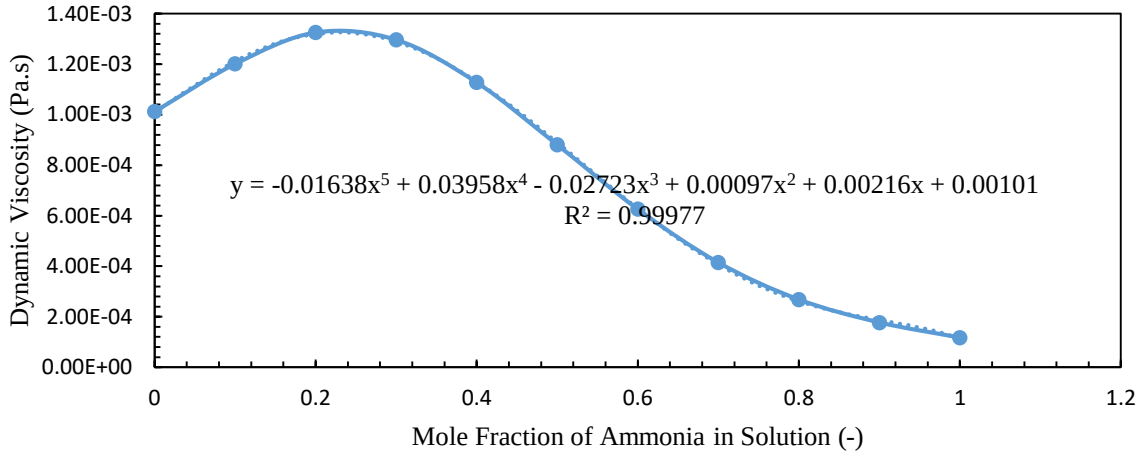

Figure 5

Equation at T = 303.15K

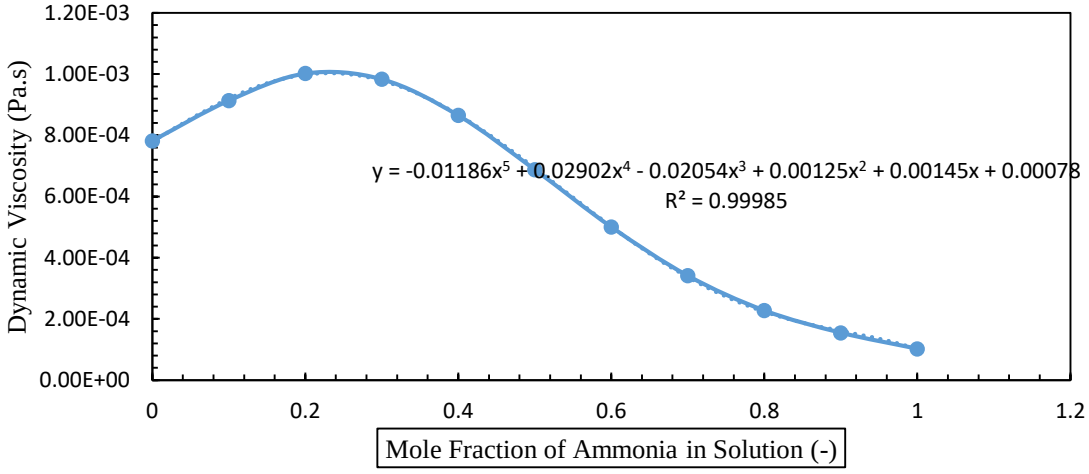

Table 2

Equations and coefficient of determination for dynamic viscosity at each temperature

Mole Fraction of Ammonia in Solution	0	0.1	0.2	0.3	0.4	0.5	0.6	0.7	0.8	0.9	1
273.15K	1.749E-03	2.122E-03	2.363E-03	2.301E-03	1.970E-03	1.500E-03	1.027E-03	6.492E-04	3.971E-04	2.478E-04	1.631E-04
Generated Equation 1 and R^2 from Microsoft Excel	$\eta = -0.030862x^5 + 0.073458x^4 - 0.048699x^3 + 0.000087x^2 + 0.004430x + 0.001742$ $R^2 = 0.999663$										
283.15K	1.328E-03	1.596E-03	1.771E-03	1.728E-03	1.490E-03	1.147E-03	7.982E-04	5.152E-04	3.233E-04	2.073E-04	1.367E-04
Generated Equation 2 and R^2 from Microsoft Excel	$\eta = -0.02263x^5 + 0.05424x^4 - 0.03656x^3 + 0.00063x^2 + 0.00313x + 0.00132$ $R^2 = 0.99971$										
293.15K	1.012E-03	1.201E-03	1.326E-03	1.297E-03	1.128E-03	8.811E-04	6.258E-04	4.144E-04	2.678E-04	1.769E-04	1.168E-04
Generated Equation 3 and R^2 from Microsoft Excel	$\eta = -0.01638x^5 + 0.03958x^4 - 0.02723x^3 + 0.00097x^2 + 0.00216x + 0.00101$ $R^2 = 0.99977$										
303.15K	7.819E-04	9.134E-04	1.002E-03	9.834E-04	8.651E-04	6.878E-04	5.004E-04	3.411E-04	2.274E-04	1.547E-04	1.023E-04
Generated Equation 4 and R^2 from Microsoft Excel	$\eta = -0.01186x^5 + 0.02902x^4 - 0.02054x^3 + 0.00125x^2 + 0.00145x + 0.00078$ $R^2 = 0.99985$										

The novel concept of proportional nodes was introduced to account for variations in the dynamic viscosity of the ammonia-water solution at different temperatures. To illustrate this method, the mole fraction with the greatest difference in dynamic viscosity was considered, which, for demonstration purposes, was assumed to be at 0.2 moles. This is main argument that a graphical illustration (figure 1) is necessary. Generally, a computer program can be generated to determine the exact mole fraction. Table 3 highlights that the dynamic viscosity decreases consistently as temperature increases, affirming the inverse relationship between temperature and viscosity, commonly observed in fluid dynamics (Holman & Gajda, 2001).

Table 3

Dynamic viscosity values of ammonia-water Solution at 0.2 wt fraction for Various Temperatures

Temperature (K) (y -value)	Dynamic Viscosity (Pa.s) (x-value)
273.15	2.363E-03
283.15	1.771E-03
293.15	1.326E-03
303.15	1.002E-03

The procedure for calculating the proportional nodes for each temperature is shown in table 4.

Table 4

Procedure for calculating the proportional nodes

Temperature (K) (y value)	Dynamic viscosity (Pa.s) (X value)	Values of proportional nodes (x values)	
273.15	2.363E-03 =A	(A-A)/(A-D)	0.0000
283.15	1.771E-03 = B	(A-B)/(A-D)	4.35E-01
293.15	1.326E-03 = C	(A-C)/(A-D)	7.62E-01
303.15	1.002E-03 = D	(A-D)/A-D)	1.0000

The equation of the proportional nodes is gotten by applying Microsoft Excel. The details are extracted from Table 4 and is shown in Table 5.

Table 5

Proportional nodes data

Temperature (K)	Nodes
273.1500	0.0000
283.1500	4.35E-01
293.1500	7.62E-01
303.1500	1.0000

The Microsoft Excel plot of table 5 is shown in figure 6.

Figure 6

Plot of Nodes data

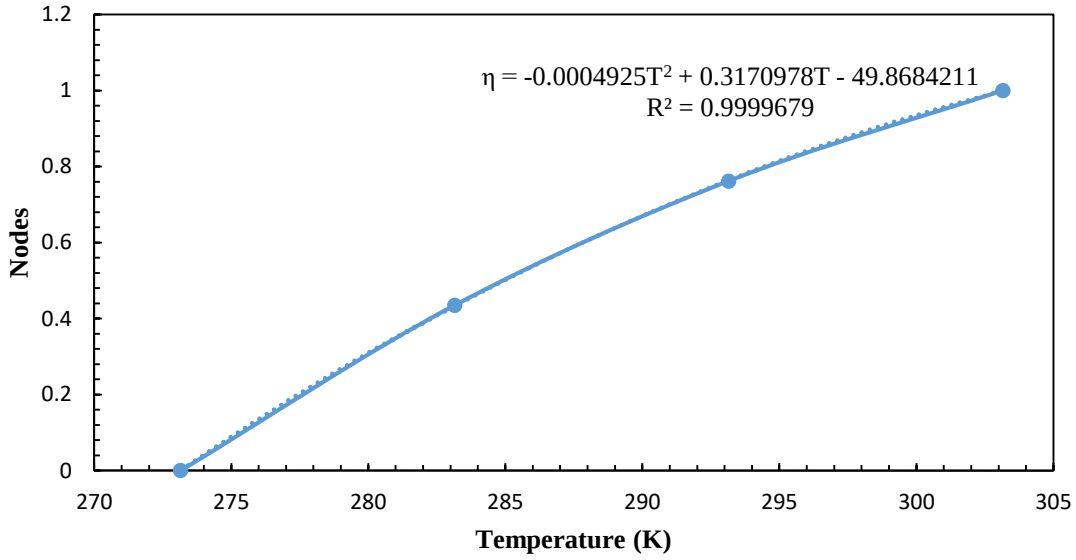

$$Nodes = -0.0004925\,T^2 + 0.3170978\,T - 49.8684211 \quad (1)$$

$$R^2 = 0.9999679$$

The proportional nodes were computed using a methodical procedure, as outlined in table 4. These nodes were then utilized to generate a second-degree polynomial as seen in equation (1), with an impressive R^2 value of 0.9999679. This polynomial represents how the viscosity changes as the temperature changes for a specific mole fraction, essentially acting as a scaling factor. The equations of each line is shown in table 2 including the proportional nodes equation. It must be stressed that for this method, the power of the polynomial should be maintained for each temperature. In addition, the Trendline Option (Microsoft Excel) should also be maintained for each process.

Therefore, the dynamic viscosity at any point within the temperature range is given by equation (2).

η (Pa.s)= (Equation of enthalpy at point where nodes =0) - [(Equation of enthalpy at point where nodes =1) – (Equation of enthalpy at point where nodes =0)] x Nodes Equation* (2)

** Please note that the sign is minus and not plus because dynamic viscosity decreases as temperature increases.*

The dynamic viscosity of ammonia-water solution can be represented by:

$$\eta\ (Pa.s) = y = (-0.030862X^5 + 0.073458X^4 - 0.048699X^3 + 0.000087X^2 + 0.00443X + 0.001742)-((-0.030862X^5 + 0.073458X^4 - 0.048699X^3 + 0.000087X^2 + 0.00443X + 0.001742)-(-0.01186X^5 + 0.02902X^4 - 0.02054X^3 + 0.00125X^2 + 0.00145X + 0.00078))x\ Nodes \quad (3)$$

or

$$\eta\ (Pa.s)=(-0.030862X^5 + 0.073458X^4 - 0.048699X^3 + 0.000087X^2 + 0.00443X + 0.001742)-((-0.030862X^5 + 0.073458X^4 - 0.048699X^3 + 0.000087X^2 + 0.00443X + 0.001742)-(-0.01186X^5 + 0.02902X^4 - 0.02054X^3 + 0.00125X^2 + 0.00145X + 0.00078))\ (-0.0004925T^2 + 0.31709775T - 49.868421081) \quad (4)$$

Simplifying the equation,

$-0.030862x^5 + 0.073458x^4 - 0.048699x^3 + 0.000087x^2 + 0.004430x + 0.001742$
-
There is a bracket here

$-0.030862x^5 + 0.073458x^4 - 0.048699x^3 + 0.000087x^2 + 0.004430x + 0.001742$ - $(-0.01186x^5 + 0.02902x^4 - 0.02054x^3 + 0.00125x^2 + 0.00145x + 0.00078)$	$*\ (-0.0004925T^2 + 0.31709775T - 49.868421081$

Subtracting first the coefficients in the bracket,

-0.030862	0.073458	-0.048699	0.000087	0.004430	0.001742
-					
-0.01186	0.02902	-0.02054	0.00125	0.00145	0.00078
=					
-0.01900	**0.04444**	**-0.02816**	**-0.00116**	**0.00298**	**0.00096**

Thus,

$-0.030862x^5 + 0.073458x^4 - 0.048699x^3 + 0.000087x^2 + 0.004430x + 0.001742$
-
There is a bracket here

$-0.01900x^5 + 0.04444x^4 - 0.02816x^3 - 0.00116x^2 + 0.00298x + 0.00096$	$*\ (-0.0004925T^2 + 0.31709775T - 49.868421081)$

Or,

$$\eta\ (Pa.s) = (-0.030862x^5 + 0.073458x^4 - 0.048699x^3 + 0.000087x^2 + 0.004430x + 0.001742) - (-0.01900x^5 + 0.04444x^4 - 0.02816x^3 - 0.00116x^2 + 0.00298x + 0.00096) * (-0.0004925T^2 + 0.31709775T - 49.868421081) \quad (5)$$

To prove that this equation satisfactory represents the data, the Percentage Difference for values from correlation and actual values, $[(\eta_{actual} - \eta_{calculated})/\ \eta_{actual}]*100.0)$, is calculated. From these values, the average percentage difference (Sum of Percentage Difference/Number of Points) is calculated. The values are presented in table 6.

Table 6

Percentage difference for dynamic viscosity values from correlations and actual values

Mole Fraction of ammonia in Solution	**0**	**0.1**	**0.2**	**0.3**	**0.4**	**0.5**	**0.6**	**0.7**	**0.8**	**0.9**	**1**
273.15K	1.749E-03	2.122E-03	2.363E-03	2.301E-03	1.970E-03	1.500E-03	1.027E-03	6.492E-04	3.971E-04	2.478E-04	1.631E-04
Calculated value from Proportional Nodes Method 273.15	0.001741086	0.002143045	0.002348	0.002283	0.001975	0.001517	0.001032	0.000632	0.000383	0.000027	0.000156
Percentage Difference $[(\eta_{actual} - \eta_{calculated})/\ \eta_{actual}]*100.0$	0.452487	-0.99175	0.634786	0.782269	-0.25381	-1.13333	-0.48685	2.649415	3.550743	-8.95884	4.353158
Generated Equation 1 and R^2 from Excel	$\eta = -0.030862x^5 + 0.073458x^4 - 0.048699x^3 + 0.000087x^2 + 0.004430x + 0.001742$ $R^2 = 0.999663$										
Mole Fraction of Ammonia in Solution	**0**	**0.1**	**0.2**	**0.3**	**0.4**	**0.5**	**0.6**	**0.7**	**0.8**	**0.9**	**1**
283.15K	1.328E-03	1.596E-03	1.771E-03	1.728E-03	1.490E-03	1.147E-03	7.982E-04	5.152E-04	3.233E-04	2.073E-04	1.367E-04
Calculated value from Proportional Nodes Method 283.15K	0.001326272	0.001615056	0.001766	0.00172	0.001497	0.001162	0.000803	0.000504	0.000314	0.000223	0.000132
Percentage Difference $[(\eta_{actual} - \eta_{calculated})/\ \eta_{actual}]*100.0$	0.130112	-1.19398	0.282326	0.462963	-0.4698	-1.30776	-0.60135	2.173913	2.876585	-7.57356	3.438186
Generated Equation 2 and R^2 from Excel	$\eta = -0.02263x^5 + 0.05424x^4 - 0.03656x^3 + 0.00063x^2 + 0.00313x + 0.00132$ $R^2 = 0.99971$										
Mole Fraction of Ammonia in Solution	**0**	**0.1**	**0.2**	**0.3**	**0.4**	**0.5**	**0.6**	**0.7**	**0.8**	**0.9**	**1**
293.15K	1.012E-03	1.201E-03	1.326E-03	1.297E-03	1.128E-03	8.811E-04	6.258E-04	4.144E-04	2.678E-04	1.769E-04	1.168E-04
Calculated value from Proportional Nodes Method 293.15K	0.001006214	0.001207676	0.001316	0.001286	0.001128	0.000887	0.000627	0.000406	0.000261	0.000186	0.000113
Percentage Difference $[(\eta_{actual} - \eta_{calculated})/\ \eta_{actual}]*100.0$	0.571739	-0.55587	0.754148	0.848111	0	-0.66962	-0.19175	2.027027	2.539208	-3135.16	3.253425

Generated Equation 3 and R^2 from Excel	$\eta = -0.01638x^5 + 0.03958x^4 - 0.02723x^3 + 0.00097x^2 + 0.00216x + 0.00101$ $R^2 = 0.99977$										
Mole Fraction of Ammonia in Solution	**0**	**0.1**	**0.2**	**0.3**	**0.4**	**0.5**	**0.6**	**0.7**	**0.8**	**0.9**	**1**
303.15K	7.819E-04	9.134E-04	1.002E-03	9.834E-04	8.651E-04	6.878E-04	5.004E-04	3.411E-04	2.274E-04	1.547E-04	1.023E-04
Calculated value from Proportional Nodes Method 303.15K	0.000780914	0.000920907	0.001	0.000098	0.000868	0.000694	0.000503	0.000337	0.000224	0.000161	0.00001
Percentage Difference $[(\eta_{actual} - \eta_{calculated})/\eta_{actual}]*100.0$	0.126103	-0.82187	0.199601	0.345739	-0.33522	-0.90142	-0.51958	1.201994	1.495163	-4.0724	2.248289
Generated Equation 4 and R^2 from Excel	$\eta = -0.01186x^5 + 0.02902x^4 - 0.02054x^3 + 0.00125x^2 + 0.00145x + 0.00078$ $R^2 = 0.99985$										

The average percentage difference for the surface (Sum of percentage deviation/Number of points) is calculated from values in table 6 and presented in table 7.

Table 7

Values of percentage deviation for various temperatures and mole fractions

	Mole Fraction										
Temp (K)	**0**	**0.1**	**0.2**	**0.3**	**0.4**	**0.5**	**0.6**	**0.7**	**0.8**	**0.9**	**1.0**
273.15	0.45249	-0.99175	0.63479	0.78227	-0.25381	-1.13333	-0.48685	2.64942	3.55074	-8.95884	4.35316
283.15	0.13012	-1.19398	0.28233	0.46296	-0.4698	-1.30776	-0.60135	2.17391	2.87659	-7.57356	3.43819
293.15	0.57174	-0.55587	0.75415	0.84811	0	-0.66962	-0.19175	2.02703	2.53921	-5.14415	3.25343
303.15	0.12610	-0.82187	0.19960	0.34574	-0.33522	-0.90142	-0.51958	1.20199	1.49516	-4.0724	2.24829

Average percentage difference for the surface ±0.2614293

The very low average percentage difference for the surface proves that the equation (5) satisfactorily represents the final expression for calculating the dynamic viscosity of the ammonia-water solution at any given temperature and mole fraction for the selected temperature range.

Assuming to increase the temperature bounds (273.15 to 423.15K) and the procedure is repeated, the results are presented.

Table 8

Dynamic viscosity of ammonia-water solution for various temperatures and mole fraction

T (K)	Mole fraction (-)										
	0	0.1	0.2	0.3	0.4	0.5	0.6	0.7	0.8	0.9	1
273.15	1.749E-03	2.122E-03	2.363E-03	2.301E-03	1.970E-03	1.500E-03	1.027E-03	6.492E-04	3.971E-04	2.478E-04	1.631E-04
283.15	1.328E-03	1.596E-03	1.771E-03	1.728E-03	1.490E-03	1.147E-03	7.982E-04	5.152E-04	3.233E-04	2.073E-04	1.367E-04
293.15	1.012E-03	1.201E-03	1.326E-03	1.297E-03	1.128E-03	8.811E-04	6.258E-04	4.144E-04	2.678E-04	1.769E-04	1.168E-04
303.15	7.819E-04	9.134E-04	1.002E-03	9.834E-04	8.651E-04	6.878E-04	5.004E-04	3.411E-04	2.274E-04	1.547E-04	1.023E-04
333.15	4.317E-04	4.758E-04	5.086E-04	5.062E-04	4.648E-04	3.938E-04	3.096E-04	2.295E-04	1.660E-04	1.210E-04	8.030E-05
343.15	3.950E-04	4.300E-04	4.569E-04	4.562E-04	4.229E-04	3.630E-04	2.896E-04	2.178E-04	1.596E-04	1.174E-04	7.800E-05
363.15	3.194E-04	3.331E-04	3.428E-04	3.379E-04	3.141E-04	2.735E-04	2.226E-04	1.705E-04	1.254E-04	9.009E-05	5.694E-05
383.15	2.681E-04	2.673E-04	2.654E-04	2.577E-04	2.404E-04	2.127E-04	1.771E-04	1.384E-04	1.022E-04	7.155E-05	4.265E-05
403.15	2.267E-04	2.141E-04	2.029E-04	1.928E-04	1.807E-04	1.636E-04	1.403E-04	1.125E-04	8.352E-05	5.656E-05	3.110E-05
423.15	1.940E-04	1.723E-04	1.536E-04	1.417E-04	1.338E-04	1.249E-04	1.114E-04	9.207E-05	6.876E-05	4.475E-05	2.200E-05

Once again, the data is depicted in graphical form as shown in figure 7, and the dynamic viscosity values at 0.2wt fraction are extracted as shown in table 9.

Figure 7

Variation of dynamic viscosity of ammonia-water solution for various mole fraction and temperatures

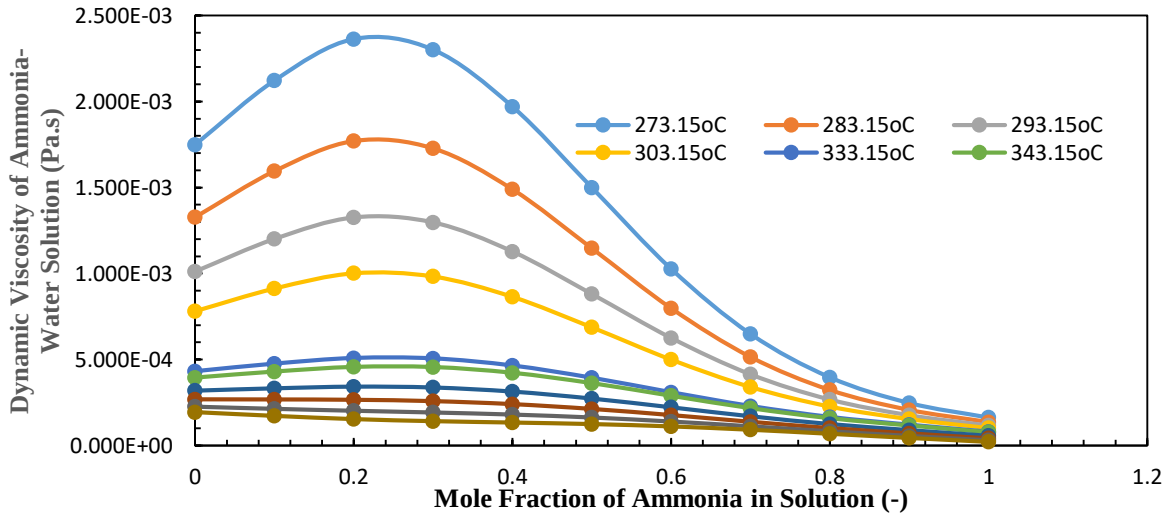

Table 9

Dynamic viscosity values of ammonia-water solution at 0.2 wt fraction for various temperatures

Temperature (K) (y -value)	Dynamic Viscosity (Pa.s) (x-value)
273.15	2.363E-03
283.15	1.771E-03
293.15	1.326E-03
303.15	1.002E-03
333.15	5.086E-04
343.15	4.569E-04
363.15	3.428E-04
383.15	2.654E-04
403.15	2.029E-04
423.15	1.536E-04

The procedure for calculating the new set of proportional nodes for each temperature is shown in table 10.

Table 10

Procedure for calculating the proportional nodes

Temperature (K) (y value)	Dynamic viscosity (Pa.s) (X value)	Values of proportional nodes (x values)	
273.15	2.363E-03 =A	(A-A)/(A-J)	0.00E+00
283.15	1.771E-03 = B	(A-B)/(A-J)	2.68E-01
293.15	1.326E-03 = C	(A-C)/(A-J)	4.69E-01
303.15	1.002E-03 = D	(A-D)/A-J)	6.16E-01
333.15	5.086E-04 = E	(A-E)/(A-J)	8.39E-01
343.15	4.569E-04 =F	(A-F)/(A-J)	8.63E-01
363.15	3.428E-04= G	(A-G)/(A-J)	0.914366
383.15	2.654E-04=H	(A-H)/(A-J)	9.49E-01
403.15	2.029E-04=I	(A-I)/(A-J)	0.977686
423.15	1.536E-04=J	(A-J)/A-J)	1.00E+00

The Microsoft Excel plot of table 10 is shown in figure 8.

Figure 8

Plot of Nodes data

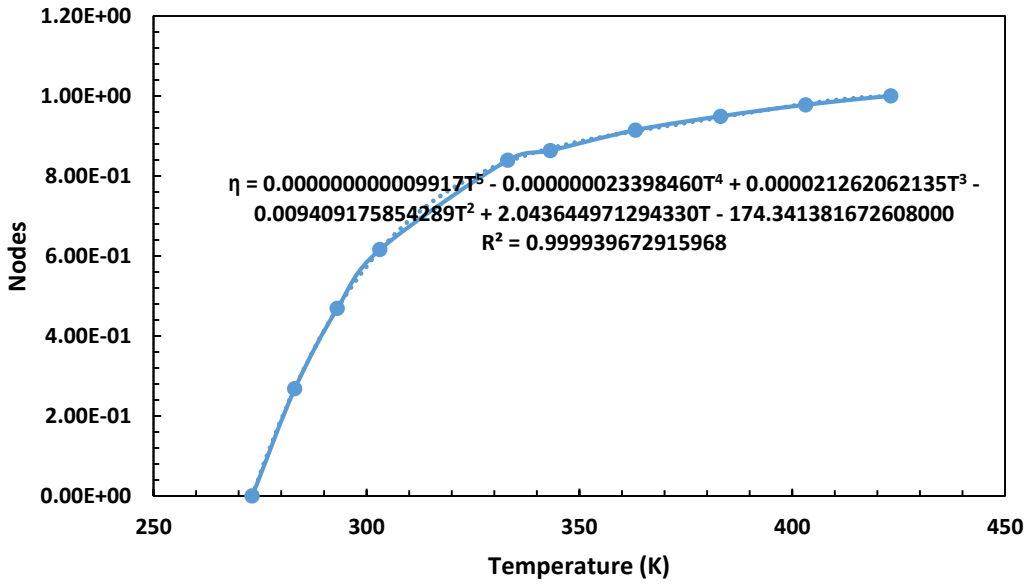

The dynamic viscosity of ammonia-water solution is calculated by following the same procedure earlier explained.

$$\eta\ (Pa.s) = (-0.030862X^5 + 0.073458X^4 - 0.048699X^3 + 0.000087X^2 + 0.00443X + 0.001742)-((-0.030862X^5 + 0.073458X^4 - 0.048699X^3 + 0.000087X^2 + 0.00443X + 0.001742)-(0.000737x^5 - 0.001389x^4 + 0.000493x^3 + 0.000246x^2 - 0.000259x + 0.000194))x\ Nodes \quad (6)$$

or

$$\eta\ (Pa.s)=(-0.030862X^5 + 0.073458X^4 - 0.048699X^3 + 0.000087X^2 + 0.00443X + 0.001742)-((-0.030862X^5 + 0.073458X^4 - 0.048699X^3 + 0.000087X^2 + 0.00443X + 0.001742)-(0.000737x^5 - 0.001389x^4 + 0.000493x^3 + 0.000246x^2 - 0.000259x + 0.000194))\ (0.000000000009917T^5 - 0.0000000233984607T^4 + 0.000021262062135T^3 - 0.009409175854289T^2 + 2.043644971294330T - 174.341381672608000) \quad (7)$$

or

$$\eta\ (Pa.s)= (-0.030862x^5 + 0.073458x^4 - 0.048699x^3 + 0.000087x^2 + 0.004430x + 0.001742)-(-0.0316x^5 + 0.074847x^4 - 0.04919x^3 - 0.00016x^2 + 0.004689x + 0.001548)*\ (0.000000000009917T^5 - 0.0000000233984607T^4 + 0.000021262062135T^3 - 0.009409175854289T^2 + 2.043644971294330T - 174.341381672608000) \quad (8)$$

To authenticate the accuracy of the correlation, average percentage deviation is calculated as shown in table 11.

Table 11

Values of percentage deviation for various temperatures and mole fractions

T (K)		Mole fraction (-)										
		0	**0.1**	**0.2**	**0.3**	**0.4**	**0.5**	**0.6**	**0.7**	**0.8**	**0.9**	**1**
2.73E+02	Actual	1.75E-03	2.12E-03	2.36E-03	2.30E-03	1.97E-03	1.50E-03	1.03E-03	6.49E-04	3.97E-04	2.48E-04	1.63E-04
	Calculated	1.74E-03	2.15E-03	2.35E-03	2.29E-03	1.98E-03	1.52E-03	1.03E-03	6.33E-04	3.84E-04	2.70E-04	1.56E-04
	% Deviation	-2.57E-01	1.20E+00	-4.19E-01	-5.91E-01	4.42E-01	1.35E+00	7.01E-01	-2.49E+00	-3.34E+00	9.10E+00	-4.22E+00
2.83E+02	Actual	1.33E-03	1.60E-03	1.77E-03	1.73E-03	1.49E-03	1.15E-03	7.98E-04	5.15E-04	3.23E-04	2.07E-04	1.37E-04
	Calculated	1.33E-03	1.61E-03	1.76E-03	1.71E-03	1.48E-03	1.14E-03	7.85E-04	4.87E-04	2.99E-04	2.09E-04	1.20E-04
	% Deviation	-1.73E-01	1.10E+00	-6.66E-01	-1.15E+00	-6.51E-01	-3.31E-01	-1.68E+00	-5.46E+00	-7.56E+00	8.44E-01	-1.22E+01
2.93E+02	Actual	1.01E-03	1.20E-03	1.33E-03	1.30E-03	1.13E-03	8.81E-04	6.26E-04	4.14E-04	2.68E-04	1.77E-04	1.17E-04
	Calculated	1.02E-03	1.22E-03	1.32E-03	1.28E-03	1.11E-03	8.65E-04	6.01E-04	3.79E-04	2.36E-04	1.64E-04	9.32E-05
	% Deviation	4.35E-01	1.52E+00	-4.22E-01	-1.30E+00	-1.41E+00	-1.88E+00	-4.02E+00	-8.47E+00	-1.18E+01	-7.42E+00	-2.02E+01
3.03E+02	Actual	7.82E-04	9.13E-04	1.00E-03	9.83E-04	8.65E-04	6.88E-04	5.00E-04	3.41E-04	2.27E-04	1.55E-04	1.02E-04
	Calculated	7.93E-04	9.35E-04	1.00E-03	9.71E-04	8.46E-04	6.63E-04	4.68E-04	3.01E-04	1.91E-04	1.31E-04	7.39E-05
	% Deviation	1.42E+00	2.31E+00	1.60E-01	-1.26E+00	-2.18E+00	-3.55E+00	-6.55E+00	-1.16E+01	-1.61E+01	-1.53E+01	-2.78E+01
3.33E+02	Actual	4.32E-04	4.76E-04	5.09E-04	5.06E-04	4.65E-04	3.94E-04	3.10E-04	2.30E-04	1.66E-04	1.21E-04	8.03E-05
	Calculated	4.52E-04	4.99E-04	5.20E-04	4.99E-04	4.40E-04	3.56E-04	2.64E-04	1.83E-04	1.21E-04	8.11E-05	4.43E-05
	% Deviation	4.64E+00	4.97E+00	2.15E+00	-1.44E+00	-5.32E+00	-9.60E+00	-1.46E+01	-2.05E+01	-2.68E+01	-3.30E+01	-4.48E+01
3.43E+02	Actual	3.95E-04	4.30E-04	4.57E-04	4.56E-04	4.23E-04	3.63E-04	2.90E-04	2.18E-04	1.60E-04	1.17E-04	7.80E-05
	Calculated	4.00E-04	4.34E-04	4.46E-04	4.28E-04	3.79E-04	3.10E-04	2.34E-04	1.65E-04	1.11E-04	7.36E-05	3.99E-05
	% Deviation	1.32E+00	8.79E-01	-2.28E+00	-6.27E+00	-1.04E+01	-1.47E+01	-1.93E+01	-2.45E+01	-3.04E+01	-3.73E+01	-4.89E+01
3.63E+02	Actual	3.19E-04	3.33E-04	3.43E-04	3.38E-04	3.14E-04	2.74E-04	2.23E-04	1.71E-04	1.25E-04	9.01E-05	5.69E-05
	Calculated	3.33E-04	3.48E-04	3.51E-04	3.35E-04	2.99E-04	2.49E-04	1.94E-04	1.41E-04	9.74E-05	6.37E-05	3.40E-05
	% Deviation	4.30E+00	4.56E+00	2.49E+00	-9.14E-01	-4.83E+00	-8.89E+00	-1.29E+01	-1.72E+01	-2.23E+01	-2.93E+01	-4.02E+01
3.83E+02	Actual	2.68E-04	2.67E-04	2.65E-04	2.58E-04	2.40E-04	2.13E-04	1.77E-04	1.38E-04	1.02E-04	7.16E-05	4.27E-05
	Calculated	2.81E-04	2.82E-04	2.78E-04	2.63E-04	2.37E-04	2.03E-04	1.63E-04	1.23E-04	8.69E-05	5.62E-05	2.96E-05
	% Deviation	4.98E+00	5.65E+00	4.76E+00	2.17E+00	-1.24E+00	-4.73E+00	-7.96E+00	-1.10E+01	-1.50E+01	-2.15E+01	-3.07E+01
4.03E+02	Actual	2.27E-04	2.14E-04	2.03E-04	1.93E-04	1.81E-04	1.64E-04	1.40E-04	1.13E-04	8.35E-05	5.66E-05	3.11E-05
	Calculated	2.34E-04	2.21E-04	2.10E-04	1.97E-04	1.80E-04	1.60E-04	1.35E-04	1.06E-04	7.72E-05	4.92E-05	2.54E-05
	% Deviation	3.02E+00	3.38E+00	3.56E+00	2.20E+00	-1.60E-01	-2.51E+00	-4.13E+00	-5.37E+00	-7.58E+00	-1.31E+01	-1.83E+01
4.23E+02	Actual	1.94E-04	1.72E-04	1.54E-04	1.42E-04	1.34E-04	1.25E-04	1.11E-04	9.21E-05	6.88E-05	4.48E-05	2.20E-05
	Calculated	2.04E-04	1.84E-04	1.68E-04	1.56E-04	1.45E-04	1.33E-04	1.17E-04	9.62E-05	7.12E-05	4.48E-05	2.29E-05
	% Deviation	5.16E+00	6.62E+00	9.53E+00	1.02E+01	8.57E+00	6.41E+00	4.96E+00	4.46E+00	3.55E+00	1.90E-01	3.95E+00

Average percentage deviation for the surface= ±08.65%

It can be seen that increasing the temperature range increases the average percentage deviation (±0.2614293 for 273.15K to 303.15K and ±08.65% for 273.15K to 423.15K). To achieve lower average percentage differences, the temperature range is divided into two, 273.15K to 303.15K and 303.15K to 423.15K. The correlation for dynamic viscosity for temperature range 273.15K to 303.15K is represented by equation (5). Following the same procedure outlined, the correlation for dynamic viscosity for temperature range, 303.15K to 423.15K, is represented by equation (9).

$$\eta = (-0.01186x^5 + 0.02902x^4 - 0.02054x^3 + 0.00125x^2 + 0.00145x + 0.00078) - ((-0.012597x^5 + 0.030409x^4 - 0.021033x^3 + 0.001004x^2 + 0.001709x + 0.000586)(-1.341883066421660E\text{-}11T^6 + 2.978411452541260E\text{-}08T^5 - 2.748924904648520E\text{-}05T^4 + 1.350381914949820E\text{-}02T^3 - 3.723844022456550E+00T^2 + 5.465803771537870E+02T - 3.336163181385320E+04)) \quad (9)$$

Average percentage Deviation = $\pm$*1.11* (9)

5. Discussion

Equations (5) and (9) satisfactorily represent the correlations for calculating the dynamic viscosity of the ammonia-water solution at any given temperature and mole fraction for the selected temperature ranges. They incorporate the polynomial equations at the boundary temperatures (273.15K, 303.15K and 423.15K), as well as the proportional nodes equations. The resulting correlations are less complex and offer robust and highly accurate models for predicting the dynamic viscosity of an ammonia-water solution under varying conditions.

The R^2 values associated with each generated equation (as shown in table 6) are consistently very close to 1, ranging from 0.999663 to 0.99985. Also, the average percentage deviation (±0.2614293 for temperature range, 273.15K to 303.15K and $\pm$ 1.11 for temperature range, 303.15K to 423.15K) is indicative of the effectiveness of the model in predicting the dynamic viscosity of ammonia-water solution. The average percentage differences between the actual and calculated dynamic viscosity values for various mole fractions and temperatures are tabulated in table 7. These percentage differences are generally very low, affirming the strong correspondence between the model's predictions and the actual measured data. Notably, the deviations are not systematic and fluctuate around zero, indicating no apparent bias in the model's predictions. These R^2 values and low average

percentage deviation further substantiate the validity and reliability of the derived model, reflecting its strong alignment with actual observations (Motulsky & Ransnas, 1987). The inverse relationship between temperature and viscosity, as indicated in the results, is consistent with existing literature on fluid dynamics (Bergman et al., 2011). For example, it has been previously established that an increase in temperature generally corresponds to a decrease in viscosity due to the increased kinetic energy of the molecules, resulting in a reduced internal resistance to flow (Incropera & DeWitt, 2002).

6. Conclusion

This study provides a comprehensive and highly accurate model for predicting the dynamic viscosity of an ammonia-water solution under varying temperatures and mole fractions. The innovative concept of proportional nodes introduced in this study allows for temperature-adaptive predictions, a significant advantage over standard polynomial fitting techniques. The very low average percentage differences between actual and calculated values (±0.2614293 for temperature range, 273.15K to 303.15K and ±1.11 for temperature range, 303.15K to 423.15K), demonstrate the model's exceptional predictive capability and reliability. Overall, this study makes a noteworthy contribution to the understanding and calculation of the correlations for dynamic viscosity of ammonia-water mixtures, promising implications for various applications where such data arrangement for mixtures exist.

Future works on this subject are encourage to explore properties such as the density of aqueous organic and inorganic solutions, the specific heat of aqueous solutions, and other thermodynamic and engineering properties of working fluids.

Acknowledgment

The authors wish to acknowledge the funding provided for this research work by Tertiary Education Trust Fund (TETFund) under the National Research Fund (NRF) Grants. REF: TETF/R&D/CE/NRF/POLY/KADUNA/VOL. 1/B5).

References

Abbas, A., Ayub, Z. H., Ismail, T., Ayub, A. H., Li, W., Khan, T. S., and Ribatski, G. (2021). Experimental study of ammonia flow boiling in a vertical tube bundle: Part 1 – Enhanced dimple tube. *International Journal of Refrigeration*. https://doi.org/10.1016/j.ijrefrig.2021.07.012

Ahmed, Z., Saleem, S., Nadeem, S., and Khan, A. U. (2020). Squeezing Flow of Carbon Nanotubes-Based Nanofluid in Channel Considering Temperature-Dependent Viscosity: A Numerical Approach. https://doi.org/10.1007/s13369-020-04981-x

Ahmadi, M., Gharyehsafa, B. M., Farzaneh-Gord, M., Jilte, R., Kumar, R., and Chau, K. (2019). Applicability of connectionist methods to predict dynamic viscosity of silver/water nanofluid by using ANN-MLP, MARS and MPR algorithms. *Engineering Applications of Computational Fluid Mechanics*. https://doi.org/10.1080/19942060.2019.1571442

Bakhtiari Manesh, P., Shahbazi, K., and Shahryari, S. (2019). Application of Grid partitioning based Fuzzy inference system and ANFIS as novel approach for modeling of Athabasca bitumen and tetradecane mixture viscosity. *Petroleum science and technology*. https://doi.org/10.1080/10916466.2018.1471488

Barkhordar, A., Ghasemiasl, R., and Armaghani, T. (2021). Statistical study and a complete overview of nanofluid viscosity correlations: a new look. *Journal of Thermal Analysis and Calorimetry*. https://doi.org/10.1007/s10973-021-10993-y

Banerjee T., H. Firouzi, and A. O. Hero (2015). Non-parametric quickest change detection for large scale random matrices. *IEEE International Symposium on Information Theory (ISIT)*, pp. 146–150, June 2015. http://arxiv.org/abs/1508.04720.

Banerjee, T. and A. O. Hero (2016). Quickest hub discovery in correlation graphs," Signals, Systems and Computers, 2016 50th Asilomar Conference on. IEEE, pp. 1248-1255.

Bergman, T. L., Lavine, A. S., Incropera, F. P., and DeWitt, D. P. (2011). *Fundamentals of Heat and Mass Transfer* (7th ed.). John Wiley and Sons.

Bhattacharjee, S., Mishra, R. B., Malkurthi, S., and Hussain, A. (2022). Numerical Modelling of Differential Pressure Sensor System for Real-Time Viscosity Measurement. *Students Conference on Engineering and Systems*. https://repository.kaust.edu.sa/bitstream/10754/685582/1/SCES_2022_final_manuscri pt.pdf

Cardona, L. F., Rojas, R. E., and Valderrama, J. O. (2019). Correlation and prediction of ionic liquid viscosity using Valderrama-Patel-Teja cubic equation of state and the geometric similitude concept. Part I: Pure ionic liquids. *Fluid Phase Equilibria*. https://doi.org/10.1016/J.FLUID.2019.04.031

Cheng, N. S. (2008). Formula for the viscosity of a glycerol-water mixture. Industrial and Engineering Chemistry Research, 47(9), 3285-3288.

Cheraghian, G., Sajadi, S., Sharifpur, M., Alanazi, A. K., Khetib, Y., and Melaibari, A. (2021). Applying Artificial Neural Network and Response Surface Method to Forecast the Rheological Behavior of Hybrid Nano-Antifreeze Containing Graphene Oxide and CopperOxide Nanomaterials. *Sustainability*. https://doi.org/10.3390/su132011505

Conde-Petit, M. (2006). Thermophysical Properties of NH3/H2O Mixtures for the Industrial Design of Absorption Refrigeration Equipment. A formulation for Industrial Use. M. Conde Engineering, Zurich, Switzerland

Dolomatov, M., Aubekerov, T. M., Koledin, O., Kovaleva, E. A., Akhtyamova, K. R., and Vagapova, E. V. (2020). QSPR model for the forecast of dynamic viscosity of arenas by the topological characteristics of molecules. https://doi.org/10.37952/ROI-JBC- 01/20-62-6-1

Eberhard, U., Hansjoerg J. Seybold, Marius Floriancic, Pascal Bertsch, Joaquin Jiménez-Martínez, José S. Andrade Jr. and Markus Holzner (May 2019). Determination of the effective viscosity of non-newtonian fluids flowing through porous media, *Frontiers in Physics*, Volume 7, https://doi.org/10.3389/fphy.2019.00071

Habibi, Mohammad Reza; Amini, Meysam, Arefmanesh, Aref, Ghasemikafrudi, Esmaeil (2019). Effects of Viscosity Variations on Buoyancy-Driven Flow from a

Horizontal Circular Cylinder Immersed in Al2O3-Water Nanofluid, *Iranian Journal of Chemistry and Chemical Engineering*, Vol. 38, No. 1, pp 212-232

Holman, J. P., and Gajda, W. J. (2001). *Experimental Methods for Engineers* (7th ed.). McGraw-Hill.

Incropera, F. P., and DeWitt, D. P. (2002). *Introduction to Heat Transfer* (4th ed.). John Wiley and Sons

Irani, M., A. Masoud, M. Babak (2019). Curve fitting on experimental data of a new hybrid nano antifreeze viscosity: presenting new correlations for non-Newtonian nanofluid, *Physica A*, 531 (2019), 10.1016/j.physa.2019.04.073

Jaadi., Z. (Oct. 2019). Everything you need to know about interpreting correlations Towards Data Science; https://towardsdatascience.com/eveything-you-need-to-know-about- interpreting-correlations-2c485841c0b8

Jayeoba, O., and Okoya, S. (2019). Analytical solutions for the flow of a reactive third-grade fluid with temperature-dependent viscosity models in a pipe.

Jouenne, S., G. Heurteux (2020). Online Monitoring for Measuring the Viscosity of the Injected Fluids Containing Polymer in Chemical Eor. Presented in *SPE Conference at Oman Petroleum & Energy Show 2020* in Muscat, Oman Society of Petroleum Engineers

Kumar, A., and Gardas, R. L. (2010). Viscosity of aqueous ammonia solution at high pressures. *Journal of Chemical Engineering Data*, 55, 3983-3986.

Kumari, M., M. Kumar, M.S. Barak (2021). Wave propagation characteristics at the welded interface of double-porosity solid and double-porosity dual-permeability materials, *Waves Random Complex Media*, 31 (6), pp. 1682-1707, 10.1080/17455030.2019.1698789

Lide, D. R. (2005). *CRC Handbook of Chemistry and Physics* (86th ed.). CRC Press.

Narayana, M., Udawattha, D. S., and Wijayarathne, U. P. L. (2019). Predicting the effective viscosity of nanofluids based on the rheology of suspensions of solid

particles. *Journal of King Saud University - Science*. https://doi.org/10.1016/J.JKSUS.2017.09.016

Ma, C., Zhiyue Gao, Jie Yang, Lin Cheng and Tianhao Zhao (2022). Calibration of Adjustment Coefficient of the Viscous Boundary in Particle Discrete Element Method Based on Water Cycle Algorithm *Water* 2022, *14*(3), 439; https://doi.org/10.3390/w14030439

Manesh, P. B., Khalil Shahbazi & Salman Shahryari (2019) Application of Grid partitioning based Fuzzy inference system and ANFIS as novel approach for modeling of Athabasca bitumen and tetradecane mixture viscosity, *Petroleum Science and Technology*, 37:14, 1613-1619, DOI: 10.1080/10916466.2018.1471488

Melaibari, Ammar, Yacine Khetib, Abdullah K. Alanazi, Goshtasp Cheraghian, Mohsen Sharifpur and Goshtasp Cheraghian (October 2021). Applying Artificial Neural Network and Response Surface Method to Forecast the Rheological Behavior of Hybrid Nano-Antifreeze Containing Graphene Oxide and Copper Oxide Nanomaterials, *Sustainability* 13(20):11505

Miyara, A., Alam, M. J., Yamaguchi, K., and Kariya, K. (2019). Development and Validation of Tandem Capillary Tubes Method to Measure Viscosity of Fluids. https://doi.org/10.11322/TJSRAE.18-47_EM_OA

Motulsky, H., and Ransnas, L. (1987). Fitting curves to data using nonlinear regression: A practical and nonmathematical review. *FASEB Journal*, 1(5), 365-374.

Mumah, S.N. (2021). Introduction of a novel curve fitting approach: The use of Proportional Nodes. *Unpublished Research and Innovation Report*. Kaduna Polytechnic, Kaduna, Nigeria

Mumah, S.N., Akande, H.F., Mudi, K.Y., Olaniyan, I.O. and Samuel, F. (2021). Correlations for Liquid and Vapour Dynamic Viscosities for Ammonia-Water Solution. *Nigerian Research Journal of Engineering and Environmental Sciences*. 6(2) 2021 pp. 596-606

Petricioli L., Humski L., Vrani M., and Pintar D. (February 25, 2020). Data Set Synthesis based on known Correlations and Distributions for Expanded Social Graph Generation. IEEE ACESS. *10.1109/ACCESS.2020.297086*

Qinghua Yang (2017). Regression. Springer International Publishing AG 2017; L.A. Schintler, C.L. McNeely (eds.), *Encyclopedia of Big Data*, 10.1007/978-3-319-32001-4_174

Rahmanifard, Hamid, Paiman Maroufi, Hamzeh Alimohamadi and Ian D. Gate (February 2021) The application of supervised machine learning techniques for multivariate modelling of gas component viscosity: A comparative study, *Fuel* 285:119146, DOI: 10.1016/j.fuel.2020.119146

Rajiv, B., Ram Natarajan and Daqun Zhang (2019). Two-stage estimation of the impact of contextual variables in stochastic frontier production function models using Data Envelopment Analysis: Second stage OLS versus bootstrap approaches, *European Journal of Operational Research*, 278(2), pp 368-384

Razmara, N., Namarvari, H., and Meneghini, J. R. (2019). A new correlation for viscosity of model water-carbon nanotube nanofluids: Molecular dynamics simulation. *Journal of Molecular Liquids*. https://doi.org/10.1016/J.MOLLIQ.2019.111438

Rezaei S, Harandi A, Moeineddin A, Ahmad Moeineddin, Bai-Xiang Xu and Stefanie Reese (2022). A mixed formulation for physics-informed neural networks as a potential solver for engineering problems in heterogeneous domains: comparison with finite element method. *Computer Methods in Applied Mechanics and Engineering*, Volume 401, Part B, 115616

Rojas, R. E., Cardona, L. F., and Valderrama, J. O. (2019). Correlation and prediction of ionic liquid viscosity using Valderrama-Patel-Teja cubic equation of state and the geometric similitude concept. Part I: Pure ionic liquids. *Fluid Phase Equilibria*. https://doi.org/10.1016/J.FLUID.2019.04.031

Shahryari, S., Bakhtiari Manesh, P., and Shahbazi, K. (2019). Application of Grid partitioning based Fuzzy inference system and ANFIS as novel approach for modeling of Athabasca bitumen and tetradecane mixture viscosity. *Petroleum science and technology*. https://doi.org/10.1080/10916466.2018.1471488

Stanovich, K. (2007). *How to Think Straight About Psychology*. Boston, MA: Pearson.

Takahashi, T., and Lin, M. C. (2019). A Geometrically Consistent Viscous Fluid Solver with Two-Way Fluid-Solid Coupling. *Computer graphics forum (Print)*. https://doi.org/10.1111/cgf.13618

Thol, M., Richter, M. (2021). Dynamic Viscosity of Binary Fluid Mixtures: A Review Focusing on Asymmetric Mixtures. *Int J Thermophys* 42, 161. https://doi.org/10.1007/s10765-021-02905-x

Udawattha, Dilan S., Mahinsasa Narayana, and Uditha P. L. Wijayarathne (July 2019), Predicting the effective viscosity of nanofluids based on the rheology of suspensions of solid particles, *Journal of King Saud University - Science*, Volume 31, Issue 3, pp 412-426

Valderrama, J., Luis Fernando Cardona and Roberto E. Rojas (May 2019). Correlation and prediction of ionic liquid viscosity using Valderrama-Patel-Teja cubic equation of state and the geometric similitude concept. Part I: Pure ionic liquids, *Fluid Phase Equilibria*, 497, DOI: 10.1016/j.fluid.2019.04.031

Wahab, Hafiz Abdul, Hussan Zeb, Saira Bhatti, Muhammad Gulistan, Seifedine Kadry and Yunyoung Nam (2020).Numerical Study for the Effects of Temperature Dependent Viscosity Flow of Non-Newtonian Fluid with Double Stratification, *Applied. Sciences.* 2020, *10*(2), 708; https://doi.org/10.3390/app10020708

Wietecha, T., and Kurzydło, P. (2019). Determination of the dynamic viscosity coefficient of the Stokes viscometer - construction of a measuring set in the Physical Laboratory of the State Higher Vocational School in Tarnów. *Science Technology and Innovation*. https://doi.org/10.5604/01.3001.0013.2885

Zare, Y., Sang Phil Park and Kyong Yop Rhee ((2019). Analysis of complex viscosity and shear thinning behavior in poly (lactic acid)/poly (ethylene oxide)/carbon nanotubes biosensor based on Carreau–Yasuda model, *Results in Physics*, 13, 102245, pp 1-8